ScienSage

Journal of Advanced Scientific Research

Available online through https://sciensage.info

ISSN
0976-9595
Research Article

SYNTHESIS OF COBALT FERRITE NANOPARTICLES AND THEIR APPLICATIONS IN HYPERTHERMIA THERAPY

Debabrata Pal

Department of Physics, Gokhale Memorial Girls' College, 1/1 Harish Mukherjee Road, Kolkata, West Bengal, India

**Corresponding author: deba.phy@gmail.com*

Received: 01-01-2023; Accepted: 02-02-2023; Published: 28-02-2023

 https://doi.org/10.55218/JASR.202314208

ABSTRACT

Co-ferrite nanoparticles have been prepared by wet chemical route using micelles. Two sets of particles with sizes of ~100 nm and ~200 nm were obtained by varying the concentration of micelles. The morphological and crystallographic study of the particles was performed by scanning electron microscope (SEM) and x-ray diffractometer respectively. To check the suitability of the co-ferrite nanoparticles in magnetic hyperthermia therapy, various magnetic measurements were carried out in presence of AC and DC magnetic fields. To investigate the suitability of the particles in hyperthermia therapy hysteresis loss of the particles under the application of AC magnetic field with various frequencies has been carried out. The parabolic nature of power loss with the frequency of the applied AC field has been verified from experimental data. From various measurements, it appeared that the particles with an average size ~100 nm have better efficiency in view of hyperthermia therapy. A large value of the specific absorption rate (SAR) was found from the ac hysteresis of the particles.

Keywords: Cobalt ferrite nanoparticles, Coercivity, Magnetic hyperthermia therapy.

1. INTRODUCTION

Research in magnetic nanoparticles (MNPs) has gained growing interest for their versatile applications in different fields like physical, chemical, biological and engineering sciences [1-3]. The physical property of the MNPs can be varied in a wide range by varying their size, shape, morphology and other parameters which opens up extensive applications of the particles in different technological areas. The synthesis technique of nanoparticles (NPs) is the most decisive factor as it determines the particles' size, shape and morphology [4]. Among various synthesis procedures such as hydrothermal [5], sol-gel [6], non-hydrolytic, thermal decomposition etc., the co-precipitation method under the wet chemical route is most convenient as it can be synthesized in water, in mild reaction conditions and require low-cost reagents [7]. Particles prepared in this method also possess good stability and ease of surface modification. The most important property of the MNPs is the tunable magnetic property which can be utilized in different ways in various technological applications. Necessary application of the MNPs can be found in electronics, for example in high-density data storage devices, sensors etc. [8]. Recently, MNPs have been expansively utilized in various biomedical devices and applications such as magnetic resonance imaging, bio-sensing, bio-separation, tissue engineering etc. [2-3]. Potential applications of the particles in magnetic hyperthermia therapy and novel drug delivery technique have also been investigated extensively [9]. The unique magnetic property of the MNPs makes them promising materials in cancer treatment from the viewpoint of practical application. As the anticancer drug is equally harmful to both cancer and healthy cell, therefore, it is required to reach the drug at the particular affected site to overcome unwanted side effects. This purpose is served by properly engineered MNPs, as the particles can be directed and manipulated by applying an inhomogeneous dc magnetic field from outside the body [10]. The MNPs produce heat under the application of ac magnetic field, enabling them to be used in magnetic hyperthermia therapy. This generated heat can also be utilized as a stimulus for controlled drug release in novel drug-delivery techniques [11]. Depending on the behaviour of magnetization reversal in an assembly of MNPs, the mechanism of heat release is classified into

three categories. These are hysteresis loss, relaxation of magnetic moments and viscus loss. The heat produced in ferromagnetic NPs by the hysteresis loss process is much higher than the other two. As ferromagnetic particles show magnetic hysteresis and superparamagnetic particles are responsible for the relaxation of magnetic moment and viscous losses, therefore ferromagnetic and superparamagnetic particles are good candidates for this purpose [12]. Generally, with the decrease in particle size, the magnetic behaviour of the MNPs changes from ferromagnetic to superparamagnetic after a critical value which depends on the nature and composition of the particles [13]. In many biological applications, small-sized superparamagnetic particles are preferred as they show a high value of magnetization when a field is applied and no magnetic moment when the field is removed. This prevents agglomeration of the particles (due to the attraction of magnetic dipole moment) and allows them to be excreted easily from the body [14]. Ferromagnetic particles are suitable for their heating effect and other magnetic properties but as the size of the particles is large compared to superparamagnetic particles, it is an issue of crucial interest because biological application demands lower size particles (within 100 nm). Therefore, a suitable balance between particle size and magnetic property is required for the MNPs for prospective use in biomedical purposes.For all those biological applications the most important and necessary criteria for the particles are biocompatibility, biodegradability and non-toxicity. However, the properties like high magnetization, good coercivity, chemical stability, easy surface modification and uniform dispersion in the colloidal medium are also required for these types of applications. Considering those aspects, magnetite (Fe_3O_4), and maghemite (γ-Fe_2O_3) are the most extensively studied MNPs as iron and their oxides can be metabolized and transported by proteins and they also exhibited the most successful results in the bio-medical area [15]. The spinal ferrites NPs, commonly MFe_2O_4 ($M = Co^{2+}$, Zn^{2+}, Mn^{2+}, Ni^{2+} etc.), are of prime interest in this field owing to their improved magnetic properties, high saturation magnetization and different types of magnetic anisotropy. $CoFe_2O_4$ has special importance among the spinel ferrites due to their excellent magnetic properties such as high coercivity, high Curie temperature, moderate saturation magnetization and high anisotropy constant. Besides these, the particles possess excellent chemical stability, electrical insulation, easy synthesis and ease of surface modification. Those properties make cobalt ferrite particles a promising candidate in biomedical applications such as MRI, hyperthermia therapy, magnetic field-stimulated drug delivery etc.

In this work, two sets of spherical Co-ferrite nanoparticles with sizes of ~100 nm and ~200 nm were prepared and they were characterized by different characterization techniques. To explore the suitability of the particles in magnetic hyperthermia therapy, various magnetic measurements were carried out in presence of AC and DC magnetic fields.

2. EXPERIMENTAL

2.1. Material and methods

Cobalt ferrite magnetic nanoparticles (CFMNPs) were prepared by the wet chemical coprecipitation method in the micellar medium. In the synthesis process, Triton X-100 (TX-100) was employed as micelles and sodium hydroxide was used as a coprecipitating agent. All the reagents, Cobalt chloride, ferric ammonium sulfate, sodium hydroxide, TX-100 were purchased from Sigma-Aldrich and were used without further purification.

2.2. Synthesis of cobalt ferrite nanoparticles

Ferric (III) ammonium sulfate (Fe^{3+}) and cobalt (II) chloride(Co^{2+}) salts were taken in 2: 1 molar ratio (1.93 g: 0.26 g). Then the salts were put in 25 ml millipore-grade water. The solution was mixed with 25 ml TX-100 surfactant solutions (0.25 mM/L). The mixture of the solution was heated and stirred continuously. When the temperature reached 353 K, 20 ml sodium hydroxide (3M) was added to it drop by drop at a constant rate keeping other parameters unchanged. The initial reddish-brown colour of the solution turned into black colour after boiling it for 1 hour. The particles formed in the solution were separated from the mixture by centrifugation method and then washed several times to remove the surfactant. Finally, the particles are dried at 313 K for 24 hours and termed as set B. The other set of particles termed as set A was prepared in the same procedure with a different micelle concentration of 0.40 mM/L.

2.3. Characterization of cobalt ferrite nano-particles

A wide-angle X-ray diffractometer, XRD, (Rigaku Miniflex II) was employed to investigate the crystalline

structures of the cobalt ferrite nanoparticles. X-ray diffraction pattern (XRD) was carried out at room temperature using Cu K_α (λ = 0.154 nm) radiation within 2θ range from 20° to 70° under 1°/min scanning rate (at 40KV & 40 mA). The surface morphological structure of the particles was studied by a scanning electron microscope (SEM, QUANTA FEG 250). A vibrating sample magnetometer (VSM, Lake Shore Model-7144) was utilized to measure DC magnetic properties of the CFMNPs at various temperatures up to a magnetic field of 1.6 T. The AC magnetic field-dependent measurements (hysteresis loop) at room temperature were carried out in our own laboratory-made AC hysteresis measurement setup.

3. RESULTS AND DISCUSSION

3.1. Structural and morphological properties

The SEM micrographs of the two sets of synthesized particles A and B have been depicted in Fig. 1(a) and (b) respectively. It is evident from those images that both sets of particles are spherical in shape. The average size/diameter of the particles is found to be ~100 nm (Fig. 1(a)) and ~200 nm (Fig. 1(b)) for sets A and B respectively.

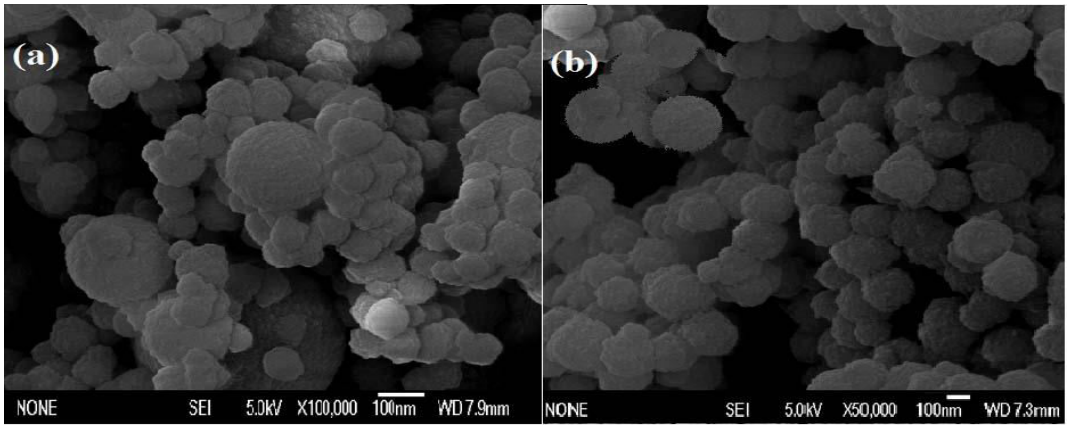

Fig. 1: SEM micrograph of the particles of size (a) 100 nm and (b) 200 nm.

The average size of the particles in set-A is smaller compared to that in set-B as the former synthesized in a higher micelles' concentration. In this synthesis process, TX-100 micelles are used as a capping agent. With the increase of TX-100 concentration, the no of micelles formed increases that affect differently during the growth of the particles by controlling the nucleation process. A higher concentration of micelles decreases the mobility of the nuclear particleswhich in turn decreases the coagulation properties results a smaller size of the particles. For lower concentrations of TX-100, the reverse situation takes place and the average particle size becomes larger.

The XRD pattern of the prepared two sets of particles with average sizes ~100 nm and ~200 nm is shown in Fig.2 (a) and (b) respectively at room temperature. The peaks of the diffraction pattern were indexed and mapped with JCPDS data (card no.- 22-1086) which confirm crystalline $CoFe_2O_4$ with expected inverse spinel structurefor both samples. No unwanted impurity phase was observed from the XRD pattern. The crystallite size of the particles for both samples was determined using Debye Scherrer's formula ($d=0.9\lambda/(\beta\cos\theta)$).The most intense peak (3 1 1) of the XRD pattern was considered to calculate the crystallite size. The samples' crystallite size (d) was found to be ~65 nm and ~70 nm for the particles of an average diameter of 100 nm and 200 nm respectively.

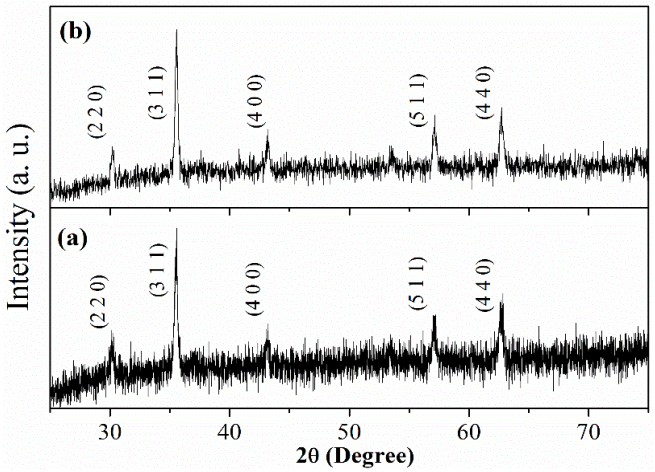

Fig. 2: X-ray diffraction pattern of the $CoFe_2O_4$nanoparticles of size (a) 100 nm and (b) 200 nm at room temperature

3.2. Magnetic properties of the $CoFe_2O_4$ nanoparticles and their application in hyperthermia therapy

In Fig. 3 the hysteresis loops (M-H curve) at room temperature of both the samples in a cycle of DC magnetic fields have been presented to study the static magnetic property of the as-synthesized Co-ferrite nanoparticles.

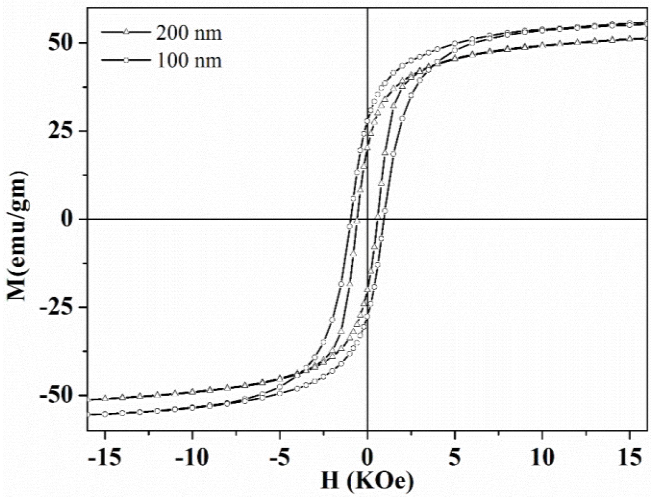

Fig. 3: DC Hysteresis loop of as-prepared particles of average size 100 nm and 200 nm at room temperature

Both the samples of particle size 100 nm and 200 nm exhibit similar types of hysteresis with slightly different coercivity (H_C) and saturation magnetization (M_S). For both the samples the crystallite size of the particles (d =65 nm and 70 nm) is larger compared to the reported value of single domain particle size of $CoFe_2O_4$ (about 20 nm) [16]. So, the particles of both samples are multi-domain nano-crystallites. In the case of multi-domain particles, magnetization is dominated by domain wall motion which causes the decrease of coercivity with the increase of crystallite size of the particles. Therefore, the coercivity of the particles of sample A (H_C=900 Oe) is higher than that of sample B (H_C=900 Oe) as the crystallite size of the former is smaller compared to the latter [17]. The increase of saturation magnetization (M_S) with the decrease in particle size may be attributed to an increase in surface spin canting [18].

In this work, the potentiality of the Co-ferrite nanoparticles in hyperthermia therapy has been investigated. In this technique, the heat generated by MNPs under the application of an ac magnetic field is used to heal the targeted cells. Depending on the behaviour of magnetization reversal in an assembly of MNPs, the mechanism/process of heat release is classified into three categories. These are hysteresis loss, relaxation of magnetic moments and viscus loss. The heat produced in ferromagnetic NPs by the hysteresis loss process is much higher than the other two [17]. Generated heat (E) due to hysteresis losses in a complete cycle of magnetization is obtained by calculating the area of the close loop under the M vs H curve (Eq. -1).

$$E = \int_{-H_{max}}^{+H_{max}} M(H)dH \qquad \text{Eq. - 1}$$

Where, M(H) is the magnetization of the MNPs and H_{max} is the maximum value of the magnetic field. Specific absorption rate (SAR) is an important parameter that is actually a measure of heat release per second and can be determined by the product of E and frequency of ac magnetic field (f) (Eq. 2).

$$SAR = E \times f \text{ (in the unit of W/g)} \qquad \text{Eq.-2}$$

Specific loss power (SLP) has the same meaning as specific absorption rate (SAR). Therefore, SLP or SAR value is a measure of the efficiency of the particles in hyperthermia therapy. Clearly, a higher SAR value implies higher efficiency.

Fig. 4 (a) shows ac magnetic hysteresis loop of 100 nm CFMNPs at a frequency of 500Hz at room temperature. A large amount of SAR value (~0.4 W/g) has been observed for these particles at that frequency. To determine the specific power loss of the particles in terms of produced heat the ac hysteresis loops of the two samples (Set-A and B) were taken within a frequency range from 50 Hz to 500 Hz and with a maximum magnetic field of 40 KA/m. The power loss (SAR) at different frequencies has been calculated from these hysteresis loops and plotted in Fig. 4 (b).The larger hysteresis loop area gives a higher value of SAR/SLP (Eq.-1 and 2).Usually, the area of the hysteresis loop is proportional to the coercivity of the particles [12].The large SAR value for the CFMNPs with size 100 nm is due to the large hysteresis loop area.For the studied particles the SLP mainly contributed from hysteresis loss as N′eel or Brown relaxation and frictional loss are not applicable for the ferromagnetic multidomain solid powder system. The hysteresis loss of this particle system increases according to the third power law on field amplitude and linearly with the field frequency [19]. So, for a fixed field amplitude, the specific power loss varies with the square of the frequency [20]. It is observed from Fig. 4 (b) that the power loss varies with the square of frequency for both

samples as expected. A parabolic nature of SLP with frequency for multidomain ferromagnetic Fe_3O_4 nanoparticles was also reported in the literature [21]. Therefore, a much higher SAR value can be obtained from these particles by increasing the field and/or frequency of the ac magnetic field within the permissible limit as per Brezovich criteria which may be utilized to destroy cancer cells by hyperthermia therapy [22].It is noteworthy that at a particular frequency the SLP for the sample of particle size 100 nm is slightly higher than that of the sample of particle size 200 nm which is due to higher coercivity and hysteresis loop area of the former. Therefore, the particles have the potential to generate heat locally under the influence of AC magnetic field and can be used inthe hyperthermia technique.

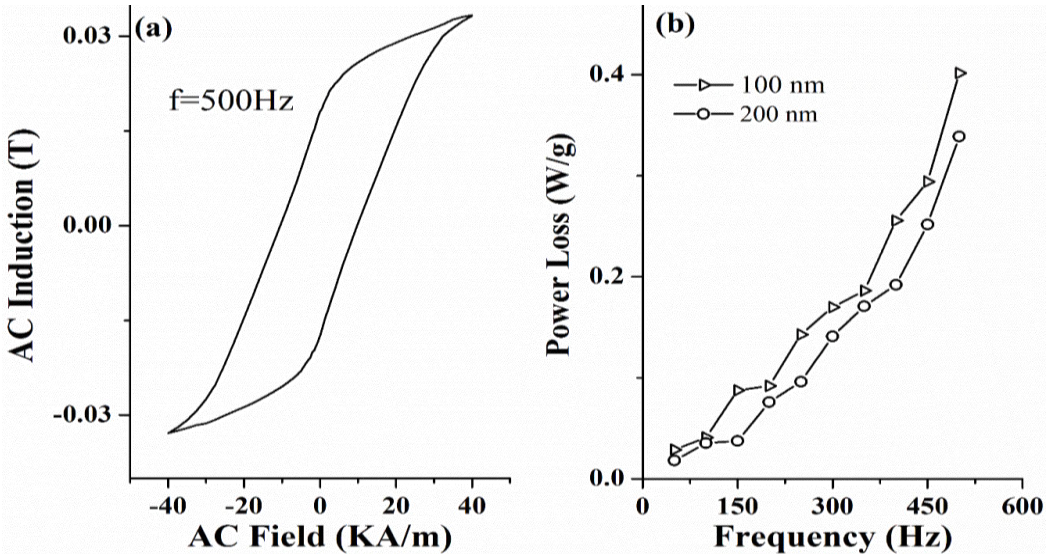

Fig. 4: (a) AC magnetic hysteresis loop at room temperature for $CoFe_2O_4$ MNPs with an average particle size of 100 nm at a frequency of 500 Hz, (b) Variation of power loss with frequency for $CoFe_2O_4$ MNPs with an average particle size of 100 nm and 200 nm

4. CONCLUSION

Cobalt ferrite magnetic nanoparticles of sizes about 100 nm and 200 nm were prepared by the wet chemical coprecipitation method in theTX-100 micellar medium. Structural characterization confirms that the particles are pure phase cobalt ferrite with inverse spinel structure. To investigate the suitability of the particles in hyperthermia therapy the SAR (Specific absorption rate) value of the CFMNPs was calculated at various frequencies. A large amount of SAR value (~0.4 W/g) has been observed for the particles of size about 100 nm at a frequency of 500 Hz. This study shows a very good competence of the particles in AC magnetic field-influenced hyperthermia therapy. In this technique, the applied field can be controlled from outside the body. Hence the technique will be minimally invasive and more effective with no or negligible unwanted side effects. However, to make this technology a useful clinical tool a large number of basic and clinical researches needs to be done.

Conflict of interest

None declared

5. REFERENCES

1. LeeSW, BaeS, TakemuraY, Shim IB, Kim TM, Kim J, et al. *J. Magn. Magn. Mater*, 2007; **310:**2868.
2. Zhang H, Li J, Hu Y, Shen M, Shi X, Zhang G.*J. Ovarian Res,* 2016; **9**(19).
3. Sun, M, Sun B, Liu Y, Shen QD, Jiang S. *Sci. Rep.,* 2016; **6**:22368.
4. Ansari SM, Sinha BB, Phase D, Sen D, Sastry PU, Kolekar YD, et al. *ACS Appl. Nano Mater*, 2019; **2(4):**1828-1843.
5. Zhou X, Shi Y, Ren L, Bao S, Han Y, Wu S, et al. *J. Solid State Chem*, 2012; **196**:138-144.
6. Sajjiaa M, Oubaha M, Prescott T, Olabi AG. *J. Alloys Compd*, 2010; **506**:400-406.
7. Liu H, Li A, Ding X, Yang F, Sun K. *Solid State Sci,* 2019; **93**:101-108.

8. Singamaneni S, Bliznyuk VN, Binek C, Tsymbal EY. *J. Mater Chem*, 2011; **21**:16819-16845.
9. Kianfar E. *Supercond J. Nov Magn*, 2021; **34**:1709-1735.
10. Liua YL, Chena D, Shanga P, Yina DC. *J. Controlled Release*, 2019; **302**:90-94.
11. Choi SW, Zhang Y, Xia Y. *Angew Chem Int Ed Engl*, 2010; **49**(43):7904-7908.
12. Dutz S, Hergt R, Murbe J, Muller R, Zeisberger M, Andra W, et al. *J. Magn. Magn. Mater*, 2007; **308**(2):305-312.
13. Cullity BD. *Introduction to Magnetic Material, 2nd ed. London: Addison-Wesley*; 1972.
14. Park JH, Saravanakumar G, Kim K, Kwon IC. *Adv Drug Deliv Rev*, 2010; **62**(1):28-41.
15. Xue P, Sun L, Li Q, Zhang L, Guo J, Xu Z, Kang Y. *Colloids and Surfaces B: Biointerfaces,* 2017; **160**:11-21.
16. Pal D, Mandal M, Chaudhuri A, Das B, Sarkar D, Mandal K. *J. Appl. Phys*, 2010; **108**:124317.
17. Pal D. *J. Adv. Sci. Res,* 2022; **13**(08):01-06.
18. Kodama RH, Berkowitz AE, McNiff Jr.EJ, Foner S. *Phys. Rev. Lett*, 1996; **77**:394-397.
19. Joshi HM, Lin YP, Aslam M, Prasad PV, Schultz-Sikma EA, Edelman R, et al. *J. Phys. Chem. C,* 2009; **113**:17761-17767.
20. Hedayatnasab Z, Abnisa F, Wan Daud WMA. *IOP Conf. Ser.: Mater. Sci. Eng*. 2018; **334**:012042.
21. Goswami MM. *Sci Rep,* 2016; **6**:35721.
22. Atkinson WJ, Brezovich IA, Chakraborty DP. *IEEE Trans. Biomed. Eng. BME*, 1984; **31**:70-75.